Dynamic Structure Mediated by Graphitelike Al Nets on the Al_2Cu (001) Surface

L. N. Serkovic Loli, É. Gaudry, V. Fournée, M.-C. de Weerd, and J. Ledieu*

Institut Jean Lamour (UMR7198 CNRS-Nancy-Université-UPV-Metz), Ecole des Mines, Parc de Saurupt, 54042 Nancy Cedex, France

(Received 9 August 2011; revised manuscript received 15 February 2012; published 3 April 2012)

A detailed study of the (001) surface of the Al_2Cu crystal using both experimental and *ab initio* computational methods is presented in this work. The combination of both approaches gives many arguments to match the surface plane with a bulk truncated surface model terminated by incomplete Al planes. The missing rows of Al atoms lead to a $2\sqrt{2} \times \sqrt{2}R\,45°$ surface reconstruction with two domains rotated by 90° from each other. *Ab initio* calculations demonstrate that the energetic cost associated with the removal of pairs of Al atoms is the lowest for the two nearest surface Al atoms (covalentlike interaction). They reveal that the remaining atomic rows of various widths are oriented according to the graphitelike Al 6^3 nets used to describe the Al_2Cu bulk structure. The surface dynamics observed at 300 K at the Al_2Cu surface is also presented. Finally, configurational and vibrational entropies are introduced to discuss the reduced surface plane density.

DOI: 10.1103/PhysRevLett.108.146101 PACS numbers: 68.35.bd, 68.37.Ef, 71.15.Mb, 71.20.Be

Most of metal surfaces have a lattice which corresponds to the bulk crystallographic plane. Merely, the interlayer spacing perpendicular to the surface shows damping oscillations around the bulk value. Exceptions are the surfaces of some 5*d*-transition metals which reconstruct to increase the packing density. More generally, surface reconstructions are observed for covalently bonded materials like semiconductors, where broken bonds left at the surface drive the reconstruction leading to a surface unit cell larger than that of the truncated bulk [1]. Covalent bonds also occur in metallic alloys. Although the bonding strength is weaker, the present work on the $Al_2Cu(100)$ surface will demonstrate that the network of such covalent bonds can dictate surface reconstruction at metallic alloy surfaces. The Al_2Cu alloy was first studied by Friauf [2] who described it as a tetragonal crystal that belongs to the $I4/mcm$ space group with a unit cell of 12 atoms (8 Al and 4 Cu atoms) and parameters $a = b = 6.04$ Å and $c = 4.86$ Å. In 2006, this alloy structure was revisited by Grin *et al.* [3] using a chemical bonding approach to understand the different models which emerged over the last 60 years to describe this Al-Cu alloy [4–6]. This last work verified Friauf's unit cell parameters ($a = b = 6.06$ Å and $c = 4.87$ Å) and also found out that this intermetallic alloy which could be first considered as a simple metal exhibits three decisive covalentlike interactions: two Al-Al bonds (d_1 and d_2 on Fig. 1) and a Cu-Al-Cu bond (d_3 on Figs. 1(a) and 1(b) and labeled d_5 in Ref. [3]). By considering the d_1 and d_2 Al-Al bonds, Nowotny *et al.* [5] defined the Al_2Cu system as interpenetrating graphitelike aluminum 6^3 nets with copper atoms positioned in the channels between the nets. A schematic of the Al graphitelike planes is shown in Fig. 1(d).

The Al_2Cu crystal has been grown by a slow cooling method which consists of heating the alloy with a nominal composition of $Al_{67.34}Cu_{32.66}$ up to 1123 K and then cooling it very slowly to reach room temperature. The crystal was oriented using back reflection Laue x-ray diffraction and was cut perpendicular to its [001] direction. The optimum preparation conditions are Ar^+ sputtering at 1 keV and then annealing the sample up to 753 K for 110 min.

The LEED pattern (Fig. 2) exhibits a surface reconstruction with a unit mesh of $a_s = 17.14$ Å and $b_s = 8.58$ Å—these parameters were obtained by calibrating the LEED with a Ag (111) surface. The bulk and surface unit cell parameters are related by $a_s = 2\sqrt{2}a$ and $b_s = \sqrt{2}a$ (with $a = b = 6.02$ Å). Therefore, the surface reconstruction has a structure of $2\sqrt{2} \times \sqrt{2}R\ 45°$ with two domains

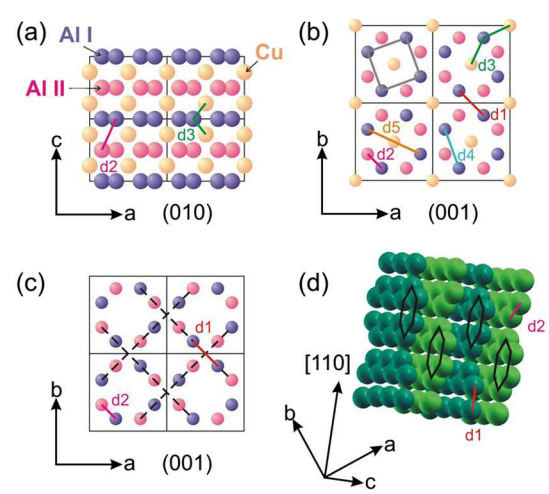

FIG. 1 (color online). Al_2Cu bulk structure (a) along the [010] and (b) [001] directions. d_1, d_2, d_4, and d_5 are bonds between Al-Al atoms and d_3 is an Al-Cu-Al bond. (c) Top view of the (001) planes. Here, Cu atoms have been removed leaving only Al atoms belonging to the graphitelike layers (broken lines in the [110] and [$1\bar{1}0$] directions). (d) Graphite-like Al nets parallel to the [110] direction.

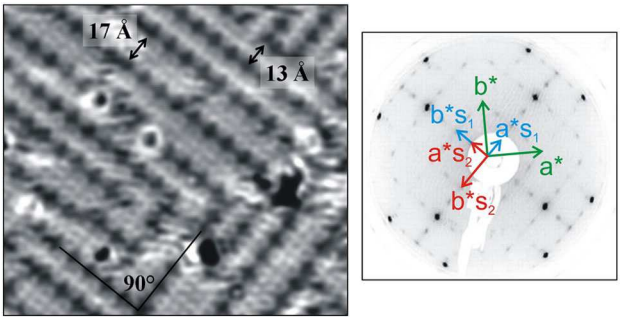

FIG. 2 (color online). STM image showing the atomic rows and the two domains rotated by 90° from each other (20×20 nm^2, $V = +2$ V, $I = 0.25$ nA). Inset: LEED pattern of the Al_2Cu (001) surface showing the $2\sqrt{2} \times \sqrt{2}R$ 45° surface reconstruction with two domains rotated from each other by 90°.

rotated by 90° from each other. All LEED patterns were taken at room temperature because no reconstruction was observed at higher temperatures.

The STM images show that the surface has a step-terrace morphology with a single step height of 2.4 Å ($c/2$). This distance corresponds to two consecutive Al or Cu layers in the bulk (twice the interlayer distance). On high resolution STM images of the terraces (Fig. 2), atomic rows (bright lines) of different widths [13, 17, and 21 Å (not shown)] distributed in two domains rotated by 90° from each other are observed (in agreement with the LEED pattern). Along the missing rows, the darkest motifs resembling diamond (see Fig. 2) are separated by 8.5 Å.

The interpretation of these experimental results requires the elaboration of a surface structural model. In the following, different surface models are considered. They are all built from bulk truncation, since the sample composition determined using angle-dependent x-ray photoelectron spectroscopy (XPS) measurements (to vary the surface sensitivity) allows us to disregard any significant surface segregation. Two different types of surface termination can then be obtained, either a pure Al or a pure Cu termination. The theoretical determination of the surface structure depends on many parameters, the most important being the concentration of the bulk alloy and the chemical potential of aluminum and copper [7]. This is far beyond the scope of this Letter. However, some simple consideration will allow us to develop a model that can account for all experimental results. Two arguments led us to consider the outermost surface plane as a termination built from a pure Al bulk layer. First, the surface terminations of a large number of aluminum-based intermetallics [8–11] results from the selection of dense Al-rich bulk planes. This is generally attributed to the lower elemental surface energy of Al compared to that of pure Cu ($\gamma_{Al(111)} = 0.75\ J \cdot m^{-2}$ and $\gamma_{Cu(111)} = 1.41\ J \cdot m^{-2}$) [12]. Second, the selection and consequently the stability of bulk planes as surface terminations will be influenced by their respective atomic density. Here, the pure Al layer is twice as dense as the Cu planes. Next, we associate the darkest motifs (diamond shaped) observed across STM images (see Fig. 2) with surface vacancies. Thus, the resulting topmost surface layer corresponds to an incomplete (missing rows) Al bulk plane. In order to determine the position of the missing surface atoms, relative formation energies of surface vacancies have been calculated within the density functional theory (DFT) framework, using the projector-augmented wave (PAW) method [13,14] within the generalized gradient approximation Perdew, Burke, and Ernzerhof proposed in Refs. [15,16]. Optimization calculations of the bulk Al_2Cu lead to (i) lattice parameters $a = 6.06$ Å and $c = 4.88$ Å, in good agreement with the experimental values and (ii) to the formation enthalpy $\Delta H_f = -0.16$ eV/atom, in good agreement with the value reported by Mihalkovič *et al.* (-0.17 eV/atom) [17] and with experimental values [18]. Relative formation energies of vacancies $\Delta E^f_{1-\mathrm{vac}} = E^f_{\mathrm{surf\text{-}vac}} - E^f_{\mathrm{bulk\text{-}vac}} = [E^{\mathrm{tot}}_{\mathrm{surf}}(1-\mathrm{vac}) - E^{\mathrm{tot}}_{\mathrm{surf}}] - [E^{\mathrm{tot}}_{\mathrm{bulk}}(1-\mathrm{vac}) - E^{\mathrm{tot}}_{\mathrm{bulk}}]$ and $\Delta E^f_{2-\mathrm{vac}} = E^{\mathrm{tot}}_{\mathrm{surf}}(2-\mathrm{vac}, d_i) - E^{\mathrm{tot}}_{\mathrm{surf}}(2-\mathrm{vac}, d_1)$ have been evaluated using 17-layers thick asymmetric slabs (Table I). Here, $E^{\mathrm{tot}}_j(n-\mathrm{vac})$ with $j = \mathrm{surf}$ or $j = \mathrm{bulk}$ is the total energy of a slab or bulk system with $n - \mathrm{vac}$ vacancies. We have checked that the energy difference for the double vacancy formation energy (the two vacancies separated by d_5) calculated using an asymmetric 17-layer thick or 15-layer thick slab is small ($\simeq 40$ meV). Since all Al surface atoms are equivalent, the formation of a single surface vacancy leads to a unique formation energy of surface vacancy. This energy is lower than the formation energy of a bulk vacancy, which can be attributed to the

TABLE I. Relative formation energy $\Delta E^f_{\mathrm{vac}}$ of vacancies in the bulk and the (001) surface of Al_2Cu. The multiple vacancies are separated by the $d_{\mathrm{vac\text{-}vac}}$ distance (referring to Fig. 1).

	1 vacancy		2 vacancies		
	Bulk ($2 \times 2 \times 2$)	Surface (2×2)	Surface (2×2)		
$d_{\mathrm{vac\text{-}vac}}$ (Å)			d_1	d_4	d_5
			2.71	3.23	4.57
$\Delta E^f_{\mathrm{vac}}{}^{1-\mathrm{vac}}$ (eV/vac)	0	−0.60			
$\Delta E^f_{\mathrm{vac}}{}^{2-\mathrm{vac}}$ (eV/vac)			0	0.31	0.35

smaller coordination number of surface atoms. The energy to create a double vacancy depends on the distance between the atoms involved. It is the lowest for two Al vacancies separated by d_1—this result is in agreement with the specific Al-Al bonding along d_1 highlighted by Ref. [3]—and greater when the distance between the two vacancies is increased.

This result partly explains the specific directions for the propagation of the empty or missing rows highlighted by the STM. Indeed, the lines of vacancies along the [110] and $[1\bar{1}0]$ directions correspond to missing Al atoms connected by a d_1 bond. As observed experimentally, symmetric equivalent positions lead to a 90° angle between the missing rows. The particular widths of the atomic rows (13, 17, and 21 Å) are related to the graphitelike Al 6^3 nets [Fig. 1(c)] used to describe the Al_2Cu structure [5]. Two consecutive graphitelike layers are separated by $d_{6^3} = \frac{1}{2} \times \sqrt{2}a$ along the [110] (respectively $[1\bar{1}0]$) directions, and shifted by d_{6^3} along the [001] direction (equivalently along [110] or $[1\bar{1}0]$ directions). Consequently, the observed widths correspond to $3 \times d_{6^3}$, $4 \times d_{6^3}$, and $5 \times d_{6^3}$. The offset (alignment) between the diamonds located on either sides of the 13 Å (17 Å) rows is explained by the offset of adjacent graphitelike 6^3 nets. The unit cell for the 17 Å rows is $2\sqrt{2} \times \sqrt{2}R\ 45°$, $3\sqrt{2} \times \sqrt{2}R\ 45°$ for the 13 Å rows, and $5\sqrt{2} \times \sqrt{2}R\ 45°$ for the 21 Å rows. However, the surface reconstruction in the LEED pattern reflects an average of the row widths, i.e., 17 Å. Furthermore, STM images indicate that the largest domains of parallel rows are made of 17 Å wide rows which should also contribute to a dominant $2\sqrt{2} \times \sqrt{2}R\ 45°$ surface reconstruction.

Figure 3 shows a good agreement between experimental and simulated STM images calculated within the Tersoff-Hamann approximation [19] based on the structural models presented on Figs. 3(b) and 3(c) for the 13 and 17 Å wide rows, respectively. A good agreement is also obtained while comparing the fast-Fourier transforms (FFT) obtained from experimental STM images and those calculated using our proposed surface model.

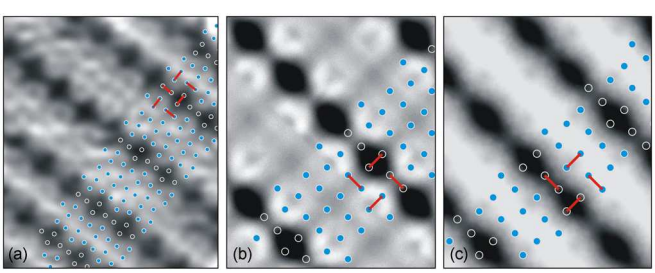

FIG. 3 (color online). (a) Experimental STM image with the "missing row model" superimposed. (b) and (c) Constant current STM images simulated using 17 Å wide (respectively 13 Å wide) row surface model at a contour of $\rho = 3.7 \times 10^{-4}\ e/\text{Å}^3$ (respectively $\rho = 7.2 \times 10^{-4}\ e/\text{Å}^3$). The LDOS is integrated from the Fermi energy ϵ_F to $\epsilon_F + 1.5$ V.

The characterization of the surface electronic structure was done using scanning tunneling spectroscopy (STS), ultraviolet photoelectron spectroscopy (UPS) and local density of states (LDOS) calculations using the 17 Å wide row surface model (Fig. 4). Significant differences are visible between the LDOS of the surface planes ($S, S-1\ldots$) and the more "bulklike" layers calculated for $S-7$ or $S-8$. The presence of common peaks in the Al sp and Cu d bulk DOS in the $[-5.5\ \text{eV};\ -4\ \text{eV}]$ region suggests a mixing of the two sets of electronic states, characteristic of a covalent character of the Al-Cu bonds. This is in agreement with the covalent Al-Cu bonding [3]. The subsurface Cu DOS contributions are of two types, corresponding to the two types of subsurface Cu atoms being either in a complete or incomplete $[CuAl_8]$ square antiprism configuration. The two types of DOS are shifted from each other by about 0.5 eV. This leads to a relatively "flat" shape of the DOS, since the number of the two types of Cu atoms are equal in the 17 Å wide row surface model. This similar weight of the different Cu states in the surface DOS (comparable to Cu $S-1$ layer having the major contribution) is qualitatively reproduced in the valence-band spectrum presented in Fig. 4. Finally, STS measurements reveal a reduction in the DOS at E_F (i.e., a pseudogap) which is present in the calculated DOS of the first Al layer (S in Fig. 4).

One peculiar feature related to this Al_2Cu system relies in the dynamics associated with the surface reconstruction. Figure 5(a) and 5(b) shows two consecutive STM images (taken 4 min. apart) recorded at 300 K on the same region of the surface under the same tunneling conditions. As a reference, the circles outline a defect common to both

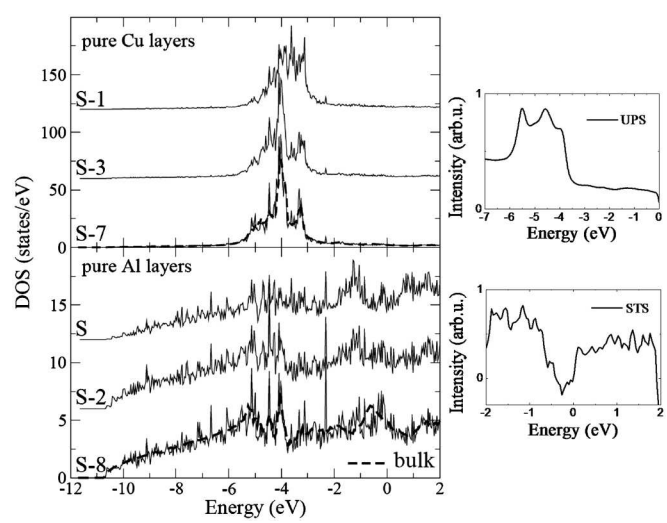

FIG. 4. DOS of the surface (S) and subsurface (S-1, S-2, S-3, ...) layers. UPS valence-band spectrum of the clean surface up to 7 eV below the Fermi level. STS measurements on the clean $Al_2Cu(001)$ reconstructed surface. The normalized dI/dV spectrum represents an average over 10^4 $I(V)$ curves before differentiation.

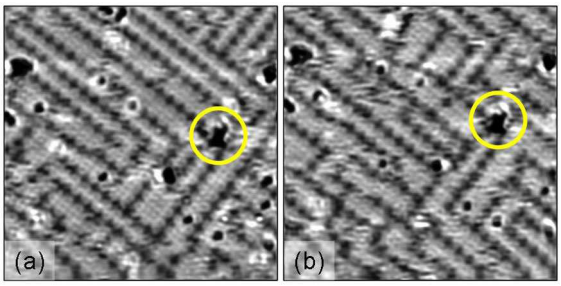

FIG. 5 (color online). Consecutive STM images taken in the same region at room temperature (20×20 nm^2, $V = +2$ V, $I = 0.25$ nA).

images. It appears that the atomic and *a fortiori* the missing rows remain highly mobile under these conditions. It is not unusual to observe a change in the atomic row width or even a change in their length and orientation. Such a dynamic surface structure has been observed systematically after each sample preparation. All atomic motions are dictated by the spacing and orientation of the graphitelike Al 6^3 nets. This surface diffusion is inhibited while scanning the sample held at 60 K. Above 300 K, the increased atomic mobility at the surface results in a (1×1) LEED pattern with a relatively high background. The $2\sqrt{2} \times \sqrt{2}R$ 45° surface reconstruction reappears upon cooling the sample back to room temperature. Hence, we believe that the surface structure described here is energetically rather than kinetically stabilized.

According to the breaking bond model [20,21], the surface energy of a dense surface plane is expected to be lower than the surface energy of a termination with surface vacancies. However, surface vacancies are observed at the surface layer. Possible explanations to this conundrum may be a surface structure stabilized by configurational entropy and/or by vibrational contribution. To gauge the thermodynamic impact of Al vacancies (missing rows), the surface structure has been modeled using a tiling approach. Two types of tiles representing each the 13 and 17 Å model have been considered. The number of each entity in the tilings is labeled $N_{i=1,2}$. Their surface energy is γ_i. Their area A_i is equal, respectively, to $A_1 = 3\alpha$ and $A_2 = 4\alpha$ where α is the area of the 1×1 surface unit cell. Here, the partition function Z has been evaluated using

$$\sum_{N_1,N_2=0}^{\infty} \frac{\Omega(N_1, N_2)}{N_1!N_2!} \exp\frac{1}{kT}(N_1\nu_1 + N_2\nu_2), \qquad (1)$$

where $\Omega(N_1, N_2)$ is the number of possible tilings, $\nu_i = -A_i\gamma_i$ is the chemical potential of a tile, and the product $N_1!N_2!$ corrects the tiles' indiscernability. In the thermodynamic limit and neglecting the long range constraints $\Omega(N_1, N_2) = 2^{N1+N2}((N1 + N2)!)$ where 2 refers to the two possible tile orientations, the configurational entropy contribution $\gamma_{\rm surf}^{\rm config}$ to the surface energy within the model is then expressed as

$$\gamma_{\rm surf}^{\rm config} = \frac{1}{xA_1 + (1-x)A_2}(-{\rm kT}\ln 2 + {\rm kT}x\ln x + {\rm kT}(1-x)\ln(1-x)),$$

with the value of $x = \frac{N_1}{N_1+N_2}$ being fixed. The $\gamma_{\rm surf}^{\rm config}$ contribution, evaluated at different temperatures (300 K/870 K), is at the most equal to 1 meV.

The evaluation of the vibrational contribution to the surface energy has been performed by the method described in Ref. [22] using the bulk vibrational frequencies $\omega_{\rm Al} = 275$ cm^{-1} and $\omega_{\rm Cu} = 146$ cm^{-1} extracted from the phonon spectra given in Wolverton *et al.* [18]. Within this model, we consider stoichiometric (bilayers) of Al_2Cu. The frequencies of surface Cu and Al atoms should vary by -10% and -33%, respectively. These values are established according to the number of broken bonds at the surface. This eventually leads to a slight stabilization of a dense Al plane at 300 K by less than 2 meV/Å^2.

Both contributions (entropic and vibrational) lead to values less than or of the same order as the numerical uncertainty in our calculations [23]. Within these limits, these two factors may contribute to the stabilization of the $2\sqrt{2} \times \sqrt{2}R$ 45° surface reconstruction as they participate to a lowering of the energy of the system.

In conclusion, *ab initio* calculations indicate that the Al-Al covalentlike bonds, identified in the bulk structure using quantum chemical calculations [3], remain stable at the surface. This work also demonstrates how the graphitelike Al 6^3 nets present in the bulk structure dictates the surface reconstruction (row spacing and domains orientations) and the dynamics at the Al_2Cu (001) surface.

M. Armbrüster and P. A. Thiel are thanked for their insightful comments. The authors acknowledge C. Chatelain for his contribution on the theoretical side. The Agence Nationale de la Recherche, reference ANR-08-Blan-0041-01, is acknowledged for its financial support. This work was supported by the HPC resources of the IDRIS under the allocation 96339 made by GENCI.

*Corresponding author.
julian.ledieu@ijl.nancy-universite.fr

[1] A. Zangwill, *Physics at Surfaces* (Cambridge University Press, Cambridge, 1988).
[2] J. B. Friauf, J. Am. Chem. Soc. **49**, 3107 (1927).
[3] Y. Grin, F. R. Wagner, M. Armbrüster, M. Kohout, A. Leithe-Jasper, U. Schwartz, U. Wedig, and H. G. von Schnering, J. Solid State Chem. **179**, 1707 (2006).
[4] P. I. Kripiakevich, *Structure Types of Intermetallic Compounds* (Nauka, Moscow, 1977) (in Russian).
[5] H. Nowotny and K. Schubert, Z. Metallkd. **37**, 17 (1946).
[6] B. G. Hyde and S. Anderson, *Inorganic Crystal Structures* (Wiley, New York, 1989).
[7] A. V. Ruban, Phys. Rev. B **65**, 174201 (2002).

[8] H. Shin, K. Pussi, É. Gaudry, J. Ledieu, V. Fournée, S. Alarcón Villaseca, J.-M. Dubois, Yu. Grin, P. Gille, W. Moritz, and R. D. Diehl, Phys. Rev. B **84**, 085411 (2011).
[9] S. Alarcón Villaseca, J. Ledieu, L. N. Serkovic Loli, M.-C. de Weerd, P. Gille, V. Fournée, J.-M. Dubois, and É. Gaudry, J. Phys. Chem. C **115**, 14 922 (2011).
[10] É. Gaudry, A. K. Shukla, T. Duguet, J. Ledieu, M.-C. de Weerd, J.-M. Dubois, and V. Fournée, Phys. Rev. B **82**, 085411 (2010).
[11] Th. Deniozou, R. Addou, A. K. Shukla, M. Heggen, M. Feuerbacher, M. Krajčí, J. Hafner, R. Widmer, O. Gröning, V. Fournée, J. M. Dubois, and J. Ledieu, Phys. Rev. B **81**, 125418 (2010).
[12] J. L. F. Da Silva, C. Stampfl, and M. Scheffler, Surf. Sci. **600**, 703 (2006).
[13] P. E. Blöchl, Phys. Rev. B **50**, 17 953 (1994).
[14] G. Kresse and D. Joubert, Phys. Rev. B **59**, 1758 (1999).
[15] J. P. Perdew, K. Burke, and M. Ernzerhof, Phys. Rev. Lett. **77**, 3865 (1996).
[16] J. P. Perdew, K. Burke, and M. Ernzerhof, Phys. Rev. Lett. **78**, 1396 (1997).
[17] M. Mihalkovič and M. Widom, http://alloy.phys.cmu.edu.
[18] C. Wolverton and V. Ozolins, Phys. Rev. Lett. **86**, 5518 (2001).
[19] J. Tersoff and D. R. Hamann, Phys. Rev. B **31**, 805 (1985).
[20] I. Galanakis, G. Bihlmayer, V. Bellini, N. Papanikolaou, R. Zeller, S. Blgel, and P. H. Dederichs, Europhys. Lett. **58**, 751 (2002).
[21] I. Galanakis, N. Papanikolaou, and P. H. Dederichs, Surf. Sci. **511**, 1 (2002).
[22] K. Reuter and M. Scheffler, Phys. Rev. B **65**, 035406 (2001).
[23] For example, the surface energy differences between various n-layers thick slabs $|\gamma_{\mathrm{Al}}^{9\text{-layers}} - \gamma_{\mathrm{Al}}^{17\text{-layers}}|$ is about 1 meV/Å^2.